ADVANCED MATERIALS
www.advmat.de

www.MaterialsViews.com

Exploring Primary Liver Macrophages for Studying Quantum Dot Interactions with Biological Systems

By *Hans C. Fischer, Tanya S. Hauck, Alejandro Gómez-Aristizábal,* and *Warren C. W. Chan**

Nanomaterial toxicity is currently a major concern and could potentially hamper the advancement of nanotechnology development. The nanotoxicology field is active and many researchers have reported on the biological responses of nanoparticles. Responses vary with nanoparticle type, properties and experimental methods.[1] A diversity of cell types to test the toxicity of nanoparticles in vitro has also been reported. Bregoli et al. recently compared primary cells with multiple immortalized cell lines and found differences in cytotoxicity between the primary cells and the cell lines.[2] Furthermore, toxicity results may differ between those of cell culture studies and in vivo animal studies. Therefore, the type of cells used for toxicity testing will impact the results and conclusions drawn regarding nanomaterial toxicity and its subsequent clinical use.

Another current research focus is to develop high-throughput in vitro testing platforms as a first step in nanotoxicity evaluation. Although in vivo toxicity characterization is the most accurate method as it takes into account all possible intracellular effects, this strategy is expensive, labor intensive, and time consuming. Cell varieties used for in vitro nanoparticle testing are intended to mirror cell types encountered in vivo. Different in vivo exposure or administration routes result in different cell types being primarily responsible for uptake. However, many in vivo studies have shown that the non-specific interactions occur with phagocytic cells that are associated with the reticuloendothelial systems. For example, resident liver macrophages, commonly called Kupffer cells (KC), are primarily responsible for in vivo uptake of intravenously dosed nanoparticles including semiconductor quantum dots (QDs),[3] nanotubes,[4] and polymer nanobeads.[5] Our aim in this study is to qualify or verify primary KCs as a suitable in vitro model by characterizing interactions of QDs with KCs freshly isolated from Sprague–Dawley rats and compare our results to previously published in vivo QD studies.[3,6]

Our study has two main aspects. The first involved preparing and characterizing QDs, and isolating and culturing primary macrophages. The second was studying QD interactions with macrophages, studying the uptake and release kinetics, metabolism, cytokine release, and cellular response to microbes. We selected diverse QD types to conduct these studies (Fig. 1A). The physical, electrophoretic, and optical properties of the QDs were characterized (Table S1, Supporting Information).

Dynamic light scattering (DLS) determined the hydrodynamic radius. Both zeta potential and gel electrophoresis verified that polyethylene glycol (PEG) and bovine serum albumin (BSA) were successfully conjugated to the blode co-polymer-coated QD (PQD) surface. QD core size measured with transmission electron microscopy (TEM) agreed with absorbance based size determination.[7] KCs were isolated (Fig. 1; Fig. S3, Supporting Information) and plated at 800 cells per mm^2 density, exposed to QD at a concentration of 0.3 nmol mL^{-1}.[8] This was equivalent to the QD concentration in vivo in a previously published study,

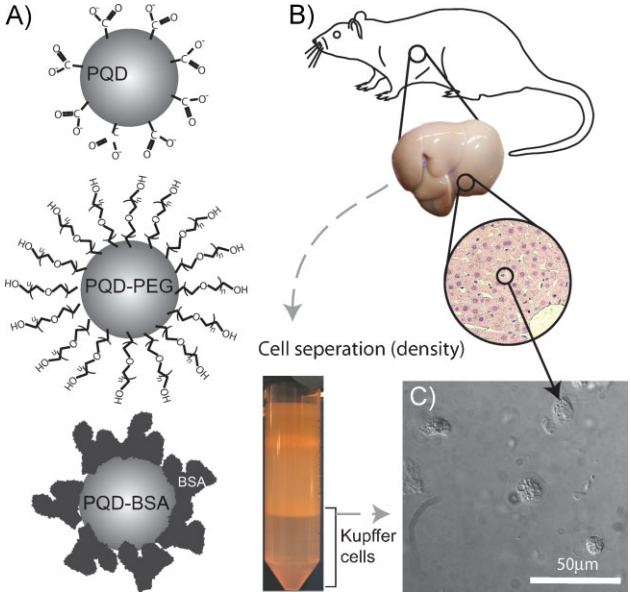

Figure 1. Quantum dot and cell model. A) Schematic of the QD types used in this study. B) Kupffer cells were isolated from rat liver using collagenase perfusion and purified by density gradient separation. C) Bright-field optical microscopy shows plated KC.

[*] Prof. W. C. W. Chan, H. C. Fischer, Dr. T. S. Hauck
Institute of Biomaterials & Biomedical Engineering
University of Toronto
Wallberg Building, Toronto, ON M5S 3G9 (Canada)
E-mail: warren.chan@utoronto.ca
Prof. W. C. W. Chan, H. C. Fischer
Department of Materials Science and Engineering
University of Toronto
Rosebrugh Building, Toronto, ON M5S 3G9 (Canada)
A. Gómez-Aristizábal
Department of Dentistry
University of Toronto
124 Edwards st., Toronto, ON M5G 1G6 (Canada)

DOI: 10.1002/adma.200904231

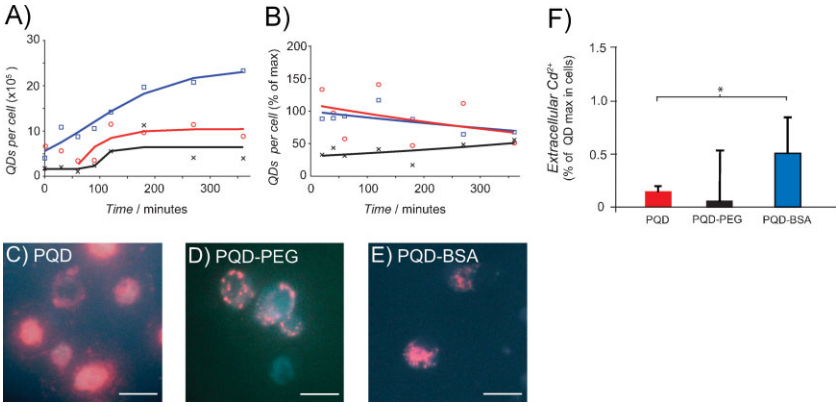

Figure 2. QD phagocytosis, exocytosis and metabolism. A) QD uptake and fit to sigmoidal function. B) Exocytosis of QD represented by the percentage of phagocytosed QD remaining in the cells after incubation in QD-free media. ($n = 3$; PQD: red, ○; PQD-PEG, black, ×; PQD-BSA, blue, □). C–E) Representative fluorescence images of QDs in KCs (at 360 min) (20 ×, λ_{ex}: 350/50 nm, λ_{em}: 430 nm LP, scale bar = 20 μm). F) Cd^{2+} release from QD breakdown, cumulative over 6 h in QD-free media ($n = 3$, $P < 0.1$).

where the injected QDs are diluted intravenously in the blood volume for a final concentration of 0.3 nmol mL^{-1}.[3]

Selected in vitro exposure conditions were scaled to agree with in vivo QD to KC ratios in vivo (1.4×10^7 QD per cell)[3] based on experimental estimates of native KC populations.[8,9] Phagocytosis experiments demonstrated in vitro capacity of 2.3×10^6, 0.9×10^6, and 0.6×10^6 QDs per cell for PQD-BSA, PQD, and PQD-PEG respectively (Fig. 2A). This showed reasonable agreement with the amount of QD taken up in vivo considering the variability present in in vivo cell population estimates. The in vivo dose uptake ranges from 5.6×10^6 to 1.4×10^7 QD/cell, depending on the surface chemistry, after 90 min.[3] Our observations mirrored published in vivo QD uptake rates that vary with different surface chemistries: BSA coating leads to 100% uptake in vivo at 60 min, and PEG surface coating results in longer circulation times and less uptake in the KCs.[10]

The mean uptake at each time point was fit to a sigmoidal curve, (Supplementary Table 2, Supporting Information) reflecting the phagocytosis process as a two stage process involving initial membrane receptor binding followed by internalization.[11,12] PQD and PQD-BSA content in KCs continued to increase over the timeframe investigated. PQD-PEG, however, demonstrated an initially slow uptake which agreed with Aggarwal et al., indicating that PEG is capable of reducing phagocytosis of QDs in vivo by shielding nanoparticles from opsonizing proteins.[13] PEG did not prevent the uptake of QD but served to limit the uptake amount to 1.6×10^5 QD/cell until 55 min, at which point uptake increased to and plateaued at 6.4×10^5 QD/cell. By reducing the presence of complement, immunoglobulins and other opsonins[14] on the QD surface, PEG mitigates the rate of initial immune recognition and phagocytosis.[15] One possible explanation for the uptake of PQD-PEG observed between 90 and 150 min after QD dosing is a change in the resistance to, or type of, proteins adsorbing to the PQD-PEG surface.[16,17] The differing kinetics between PQD, PQD-BSA and PQD-BSA uptake may indicate differences in cellular response such as receptor specificity and availability,[18] and adsorbed protein cross-section.[16] We speculate that nanomaterial properties are the main contributors to these differences. Future studies in our lab aim to identify and correlate these properties to cellular response.

Chithrani et al. show that nanoparticles are exocytosed after cellular uptake.[19] Contrastingly, Jackson et al. show intracellular sequestering.[20] Some decrease of intracellular QD occurred in vitro with KC (Fig. 2B). Exocytosis data are presented as the percent of maximum observed intracellular QD (after 6 h of QD exposure and uptake) remaining after time t in fresh media (no QD). We fit our data to a first order decay.[21] Exocytosis clearance half-lives were $t_1/_2 = 9.5$ and 12.6 h for PDQ and PQD-BSA respectively. PQD-PEG, however, showed no decrease of intracellular QDs.

Fluorescence images of cells incubated with QDs show luminescence after 12 h (Fig. 2C–E), suggesting that a majority of QD remained present and intact. The degradation of the QDs leads to loss of fluorescence and broadening of the emission spectra.[22] To quantify QD metabolism, we measured Cd^{2+} in culture media with ICP-MS after filtering the media with 10 kDa membrane to remove any intact QDs. Mancini et al. showed QDs break down in hypochlorous acid, which is commonly encountered by QDs intracellularly.[23] Given this evidence of breakdown, understanding the residence time in such an environment is of importance; however, only a very small part of the decrease in intracellular QD reported here could be attributed to QD metabolism and associated Cd^{2+} release. QD breakdown amounted to (0.15 ± 0.05)% and (0.5 ± 0.3)% of phagocytosed QD for PQD and PQD-BSA, respectively. In comparison, 39% (PQD) and 28% (PQD-BSA) were intact when released from the KC. The degradation observed is in agreement with recent studies.[6,23,24] Further, the extent of this QD degradation (Fig. 2F) was dependent on the QD surface chemistry. In these studies, the metallic species were released into an extracellular environment but in vivo, the Cd^{2+} would be released in the liver or be free to circulate. This is a potential concern since Cd^{2+} can compromise hepatocyte health.[25] Our data demonstrated that QD were sequestered but digest to their elemental components at a slow rate. In this case, primary KC provided an excellent in vitro cell model to characterize kinetics of QDs in vivo.

In vivo QD trajectory is compounded by the fact that KC migrate to lymph nodes,[26] and exhibit a 14 month average life span in vivo.[9] Our results show that PQD and PQD-BSAs did not elicit cytotoxicity, tested by quantifying the increase of membrane leakage of the cytosolic enzyme glucose-6-phosphate dehydrogenase (G6PD) into media. PQD-PEG caused a slight increase after exposure (Fig. 3A). Comparatively, metabolic function of the KCs was not compromised by QD exposure but an increase in metabolic activity. In the selected media, KCs do not proliferate[27] but the fluorescence signal for resazurin (Fig. 3C) and 3-(4,5-dimethylthiazol-2-yl)-2,5-diphenyltetrazolium bromide (also known as MTT) increased (see the Supporting Information). These compounds get modified, which can be

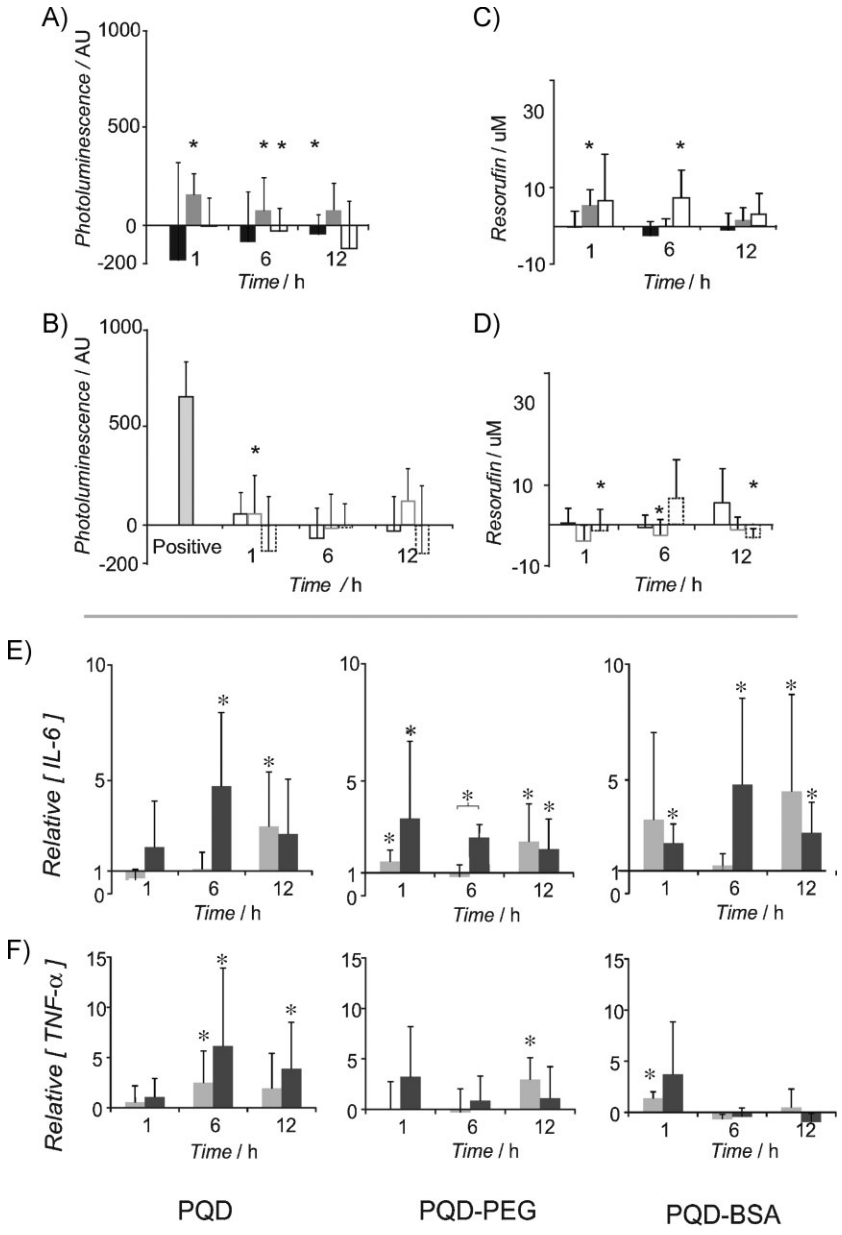

Figure 3. Kupffer cell response. A) Cytotoxicity response to QD exposure (G6PD assay). B) Corresponding controls of QD vehicle (dose with the QDs removed). C) Cellular metabolic activity in response to QD exposure. D) Corresponding QD vehicle controls. (PQD, ■; PQD-PEG, ■; PQD-BSA, □; Vehicle controls: PQD, black outline; PQD-PEG, grey outline; PQD-BSA, dashed outline). Values are the mean of the difference from untreated cells. ($n = 3$, $P < 0.05$). Measuring cytokine - E) IL-6 and F) TNF-α - concentration in response to QD and QD vehicle exposure. (QD, ■; dose vehicle, ■) Values are normalized to expression levels in untreated cells ($n = 3$, $P < 0.1$). Error bars are S.D.

measured by a change in the fluorescence properties, in the presence of metabolically active cells.

Macrophages confronted with a pathogen or foreign material release cytokines to recruit additional immune resources. We measured cytokine activation, specifically quantifying pre-inflammatory cytokines IL-6, TNF-α (Fig. 3), and IL-1β. These three cytokines contribute to acute phase response in the liver. This response involves altering plasma protein composition, which are central to tagging foreign particles for phagocytosis.[14] Individually, IL-6 is involved in lymphocyte activation that can lead to increased antibody production. Some increase in IL-6 was observed in response to each of the QD surface chemistries. We found a 4.8-fold increase for PQD at 6 h, a 3.3- and 2.0-fold increase for PQD-PEG at 1 and 6 h respectively, and a 2.2-, 4.8-, and 2.7-fold increase for PQD-BSA at 1, 6, and 12 h respectively, compared to untreated cells. An increase was also observed in response to the QD vehicle incubation in some cases. Only PQD-PEG at 6 h elicited a response significantly different that its corresponding QD-vehicle control. A substantial increase in IL-6 would suggest the presence of an adaptive response but to confirm this, a detailed in vivo study is needed. TNF-α activates endothelium to induce macrophage binding and exit from blood vessel at infection sites. KC are able to recruit dendritic cells[28] and blood monocytes through cytokine release in response to colloids that cause inflammation.[29] Some significant increases in TNF-α release were observed for PQD though not significantly different than QD vehicle controls. Lee et al. also reported TNF-α elevation both in vivo and in vitro in response to QD.[30] No increase in IL-1β was observed relative to untreated cells (see the Supporting Information). Based on these results, it was evident that some KC activation response occurred, and that more detailed immunogenic assessment of QD is necessary. In comparison, histology shows no signs of inflammation in response to in vivo QD exposure.[6] The slight increases in cytokine expression relative to untreated cells observed here might not be sufficient for observation of histological changes in the liver after QD exposure.

Lastly, we assessed whether the intracellularly sequestered QDs in KC influenced the cell's phagocytic function. KC showed no post-QD exposure phagocytic impairment, as demonstrated by a comparable uptake of fluorescently labeled inactive *E. coli* bacteria by KC with and without QDs (Fig. 4).

In summary, we demonstrated the use of KCs to study QD uptake, and show that it mimics that of in vivo studies, suggesting the KCs could be used for the initial screening of nanomaterial behavior in vivo. As nanomedicine and nanotoxicology research continues, the number of nanomaterials parameters to be examined remains prohibitively large. Thus, the development of novel high-throughput technologies is required to assess and evaluate nanomaterial cell interactions[31] which can serve as screening tools to narrow down the nanomaterial parameters for

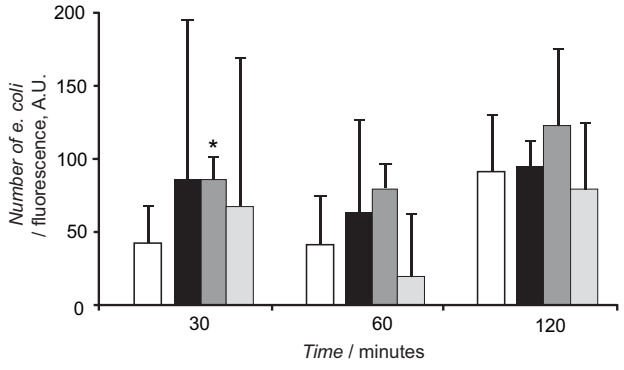

Figure 4. Phagocytic function. The effect of intracellular QD on the phagocytosis of *E. coli*. In no instance did PQD (■), PQD-PEG (■) or PQD-BSA (■) reduce the ability of KCs to phagocytose Alexa-488 labeled *E. coli*. The amount within the cells was statistically equivalent to or greater than untreated cells (□) in all conditions. ($P < 0.05$) Error bars are S.D.

more focused traditional in vivo investigations.[32] Selection of cell types to use for such testing still requires optimization to ensure accuracy across the entire breadth of nanoparticle types and exposure routes. Isolated Kupffer cells are capable of providing results that reflect in vivo observations, and we suggest that KC be included in future high throughput studies of nanoparticles that are introduced into the body intravenously.

Experimental

Quantum Dot Preparation: Details of synthesis, conjugation and characterization can be found in the Supporting Information.

ICP-MS Sample Analysis: See the Supporting Information.

Primary Kupffer Cell Isolation: Primary Kupffer cells were collected from male Sprague-Dawley rats according to Smedsrød et al. [8]. All animal handling was in accordance with university policy, under approved protocol #20006891. See the Supporting Information.

Endocytosis and Exocytosis: Primary Kupffer cells (0.2×10^6 cells per well) were plated in 24-well black body imaging plates (Genetix), and exposed to QDs (30 nmol/mL) in in vitro culture. The cells were washed thoroughly, counted, and analyzed for Cd content with ICP-MS at various time points.

Exocytosis was measured by incubating the cells with QD for 6 h, washing, exchanging the media, and then analyzing the cells with ICP-MS at various time points, for the quantity of QD remaining in the cells. Intracellular QD was quantified by subtracting non-specific adsorption to the plate (QD incubated in BSA-coated/glutaraldehyde crosslinked wells, with media, without cells) from the total phagocytosed QD measured.

For both endocytosis and exocytosis data, cadmium content was scaled to amount per cell, using the cell count numbers of individual wells acquired using the Cellomics system. This accounted for variation in plated cell number in each well.

Quantifying Metabolism: KC were incubated with QD for 6 h, washed thoroughly and provided with fresh media. After 6 h, the media was collected (150 μL) and filtered through a 10.0 kDa NMWL filter-plate (Ultracel-10, Millipore) at 3000*g* for 1 h to remove any intact QDs. The Cd^{2+} concentration of the filtrate was measured using ICP-MS. Control values from any QD Cd^{2+} contribution were subtracted.

Cytotoxicity and Immune Activation: Conjugated QDs were solvent exchanged using Amicon ultra 10 kDa MWCO and rediluted to 1 μM in fresh PBS. The filtrate ("QD vehicle") was retained as a control. Plated KCs were incubated with both QD and QD vehicle for 1, 6, and 12 h and the cellular metabolism (MTT and rezasurin (Molecular Probes)), and membrane damage (G6PD release, Molecular Probes) were tested. Each was tested according to kit protocol. Fluorescence data were analyzed with ImageJ. The release of pre-inflammatory cytokines, IL-1β, IL-6, and TNF-α, was measured using ELISA kits from Invitrogen by analyzing media, filtered with a 10 kDa filter plate, which was collected from cells incubating with QD and QD vehicle for 1, 6, and 12 h.

Bacteria Uptake: Post QD exposure to KC was exposed to inactive *E. coli*-Alexa Fluor-488 (Bioparticles, Invitrogen) preincubated in rat serum (Sigma). The cells were washed thoroughly to remove excess *E. coli*, treated with trypan blue (100 μL, 250 μg/mL, in PBS) for 5 min to quench fluorescence from any remaining extracellular *E. coli* [33], imaged on a Kodak fluorescent imaging system and quantified with ImageJ.

Statistics: Endocytosis and Exocytosis data was fit to sigmoidal and monoexponential functions respectively (Matlab). Equation coefficients and fit statistics are presented in the Supporting Information. Metabolism, cytotoxicity, cytokine and bacteria uptake experiments were analyzed using the Wilcoxon rank sum test (Matlab).

Acknowledgements

We acknowledge CIHR (RMF72551), NSERC (fellowship for HF, TSH), CFI, OIT, and KM Hunter Foundation (TSH) for financial support; Dr. Vladimir I. Baranov and his colleagues for their assistance with ICP-MS; Dr. Peter Zandstra for Cellomics analyses; and Dr. Julie Audet, Aziza Manceur, and Dr. Travis Jennings for flow cytometry assistance. A.G.-A. is a member of the research group of Dr. John E. Davies. Supporting Information is available online from Wiley InterScience or from the author.

Received: December 10, 2009
Published online: May 20, 2010

[1] R. Hardman, *Environ. Health Perspect.* **2006**, *114*, 165.
[2] L. Bregoli, F. Chiarini, A. Gambarelli, G. Sighinolfi, A. M. Gatti, P. Santi, A. M. Martelli, L. Cocco, *Toxicology* **2009**, *262*, 121.
[3] H. C. Fischer, L. Liu, K. S. Pang, W. C. W. Chan, *Adv. Funct. Mater.* **2006**, *16*, 1299.
[4] Z. Liu, C. Davis, W. Cai, L. He, X. Chen, H. Dai, *Proc. Natl. Acad. Sci. USA* **2008**, *105*, 1410.
[5] D. E. Owens, III, N. A. Peppas, *Int. J. Pharm.* **2006**, *307*, 93.
[6] T. M. Hauck, R. E. Anderson, H. C. Fischer, S. Newbigging, W. C. W. Chan, *Small* **2009**, *6*, 138.
[7] W. W. Yu, L. Qu, W. Guo, X. Peng, *Chem. Mater.* **2003**, *15*, 2854.
[8] B. Smedsrød, H. Pertoft, *J. Leukocyte Biol.* **1985**, *38*, 213.
[9] L. Bouwens, M. Baekeland, R. De Zanger, E. Wisse, *Hepatology* **1986**, *6*, 718.
[10] R. S. H. Yang, L. W. Chang, J.-P. Wu, M.-H. Tsai, H.-J. Wang, Y.-C. Kuo, T.-K. Yeh, C. S. Yang, P. Lin, *Environ. Health Perspect.* **2007**, *115*, 1339.
[11] F. C. Hay, O. M. R. Westwood, *Practical Immunology*, Blackwell Science, Oxford **2002**.
[12] S. Shirato, C. G. Murphy, E. Bloom, L. Franse-Carman, M. T. Maglio, J. R. Polansky, J. A. Alvarado, *Invest. Opthamol. Visual Sci.* **1989**, *30*, 2499.
[13] P. Aggarwal, J. B. Hall, C. B. McLeland, M. A. Dobrovolskaia, S. E. McNeil, *Adv. Drug Delivery Rev.* **2009**, *61*, 428.
[14] T. Cedervall, I. Lynch, M. Foy, T. Berggard, S. C. Donnelly, G. Cagney, S. Linse, K. A. Dawson, *Angew. Chem, Int. Ed.* **2007**, *46*, 5754.
[15] M. A. Dobrovolskaia, S. E. McNeil, *Nat. Nanotechnol.* **2007**, *2*, 469.
[16] T. Cedervall, I. Lynch, S. Lindman, T. Berggard, E. Thulin, H. Nilsson, K. Dawson, S. Linse, *Proc. Natl. Acad. Sci. USA* **2007**, *104*, 2050.
[17] M. Lundqvist, J. Stigler, G. Elia, I. Lynch, T. Cedervall, K. A. Dawson, *Proc. Natl. Acad. Sci. USA* **2008**, *105*, 14265.

[18] W. Jiang, B. Y. S. Kim, J. T. Rutka, W. C. W. Chan, *Nat. Nanotechnol.* **2008**, *3*, 145.
[19] B. D. Chithrani, A. A. Ghazani, W. C. W. Chan, *Nano Lett.* **2006**, *6*, 662.
[20] H. Jackson, O. Muhammad, H. Daneshvar, J. Nelms, A. Popescu, M. A. Vogelbaum, M. Bruchez, S. Toms, *Neurosurgery* **2007**, *60*, 524.
[21] J. M. Besterman, J. A. Airhart, R. B. Low, D. E. Rannels, *J. Cell Biol.* **1983**, *96*, 1586.
[22] J. A. Lee, S. Mardyani, A. Hung, A. Rhee, J. Klostranec, Y. Mu, D. Li, W. C. W. Chan, *Adv. Mater.* **2007**, *19*, 3113.
[23] M. C. Mancini, B. A. Kairdolf, A. M. Smith, S. Nie, *J. Am. Chem. Soc.* **2008**, *130*, 10836.
[24] J. A. J. Fitzpatrick, S. K. Andreko, L. A. Ernst, A. S. Waggoner, B. Ballou, M. P. Bruchez, *Nano Lett.* **2009**, *9*, 2736.
[25] A. M. Derfus, W. C. W. Chan, S. N. Bhatia, *Nano Lett.* **2004**, *4*, 11.
[26] M. J. Hardonk, F. W. J. Dijkhuis, J. Grond, J. Koudstaal, S. Poppema, *Virchows Archiv B* **1986**, *51*, 429.
[27] R. M. J. Hoedenmakers, G. L. Scherphof, T. Daemen, *Hepatology* **1993**, *19*, 666.
[28] K. Matsuno, H. Nomiyama, H. Yoneyama, R. Uwatoku, *Dev. Immunol.* **2002**, *9*, 143.
[29] L. Bouwens, E. Wisse, *J. Leukocyte Biol.* **1985**, *37*, 531.
[30] H. A. Lee, T. L. Leavens, S. E. Mason, N. A. Monteiro-Riviere, J. E. Riviere, *Nano Lett.* **2009**, *9*, 794.
[31] R. F. Service, *Science* **2008**, *231*, 1036.
[32] S. Y. Shaw, E. C. Westly, M. J. Pittet, A. Subramanian, S. L. Schreiber, R. Weissleder, *Proc. Natl. Acad. Sci. USA* **2008**, *105*, 7387.
[33] C. P. Wan, C. S. Park, B. H. S. Lau, *J. Immunol. Methods* **1993**, *162*, 1.